Zhijun Fu
Xiang Zhang
Zhigang Zhang ✉
Dengfeng Zhao
Yuming Yin

https://doi.org/10.21278/TOF.483061123
ISSN 1333-1124
eISSN 1849-1391

A REVIEW ON MODELLING AND CONTROL OF MAGNETORHEOLOGICAL DAMPERS

Summary

The inherent nonlinear nature caused by the hysteresis characteristics of the force-displacement and force-velocity relationships poses a challenge to the modelling and control of magnetorheological (MR) dampers. In this review, two types of modelling methods, parametric modelling and non-parametric modelling, are critically reviewed and discussed, with a focus on how to improve modelling accuracy. Although the force-displacement behaviour is well represented by most of the proposed dynamic models for MR dampers, no simple parametric models with high accuracy can be found for MR dampers. In addition, non-parametric modelling methods can improve the accuracy of the model, but the complexity of the model and the computational burden cause difficulties in designing the closed-loop controller. Finally, the control methods based on different modelling methods are discussed, and future research directions are also recommended.

Key words: *magnetorheological damper, model, control strategy*

1. Introduction

The MR damper as shown in Figure 1 is an excellent damping device used to mitigate the adverse effects of equipment when subjected to shock and vibration [1]. Due to the advantages of the large viscosity control range, relatively low cost, lower power consumption, fast response time (a millisecond range) [2], and a smaller size [3, 4], an MR damper is widely used in vehicles, construction, and medicine [5, 6, 7, 8]. MR fluid is an innovative type of intelligent material that was first discovered by Rabinow [9]. This material is mainly composed of a liquid carrier (accounting for about 50-80% by volume) [10], magnetic particles (about 1-10μm in size) [11], and some other attachments. In the absence of an external magnetic field, MR fluids exhibit Newtonian-like properties [12, 13], in which magnetic particles can flow freely in the liquid [14]. However, in the presence of a magnetic field, there is a mutual interaction among the magnetic particles, forming a chain structure that transforms fluid properties into a state with considerable yield stress, which is known as the magnetorheological effect, as shown in Figure 2.

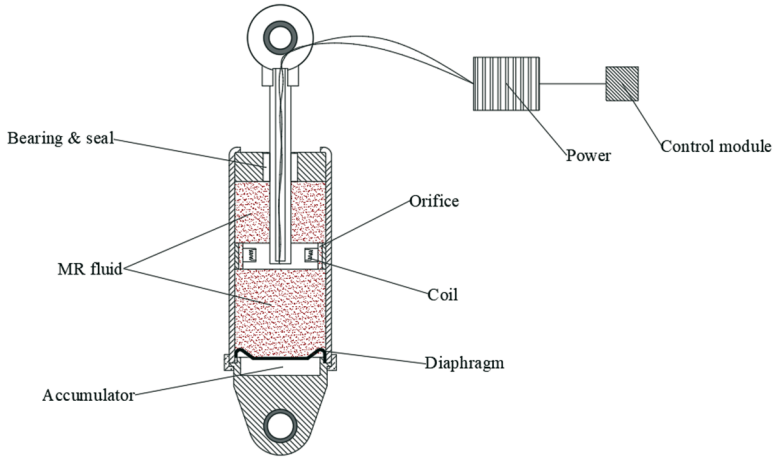

Fig. 1 Structure of MR damper

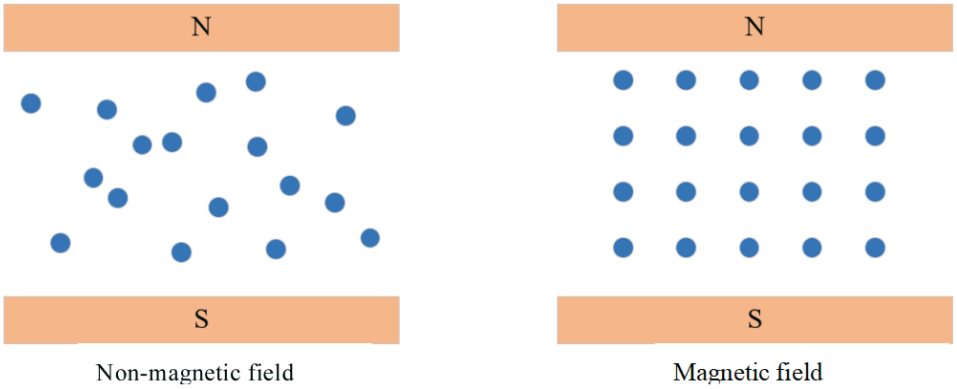

Fig. 2 Magnetorheological effect

The classic MR fluid operation modes are divided into four types: the flow (valve) mode, the shear mode, the squeeze mode and the pinch mode [15-18], and their structures are shown in Figure 3. It is worth mentioning that only the flow (valve) and squeeze modes have been commercialized, and the two other modes are still in the research stage [19]. By controlling the internal magnetic field, the damping force of the MR damper is adjusted to change the viscosity of the MR fluid [20, 21], thereby achieving the control of the damper. An increase in current in the coil leads to an increase in the magnetic field, which in turn increases the resistance of the MR fluid flowing through the orifice, thereby increasing the damping force. On the other hand, a decrease in current will reduce the damping force. In addition, if the control module or power supply fail, the MR damper will become a passive damper and continue to provide basic vibration damping functions [22], which gives the MR damper good controllable continuity in both on and off states.

However, the complex rheological properties of MR fluids make it difficult to model their dynamic properties [23]. Therefore, many MR damper models considering hysteresis characteristics have been studied, such as the Bingham model [24,25], the Bouc-Wen model [26], the neural network model [27], etc. These models can be classified as parametric and non-parametric models based on different modelling methodologies. In addition, the control strategies can be divided into the model-based control strategy and the soft computing-based control strategy. The model-based control strategy is applicable to a type of situation where an accurate model of the controlled object has been established, such as the Clipped optimal control [28] or the Lyapunov control algorithm [29, 30]. When it is difficult to establish an

accurate model, control strategies based on soft computing will be adopted, such as the neural network control [31] and the fuzzy control [32, 33].

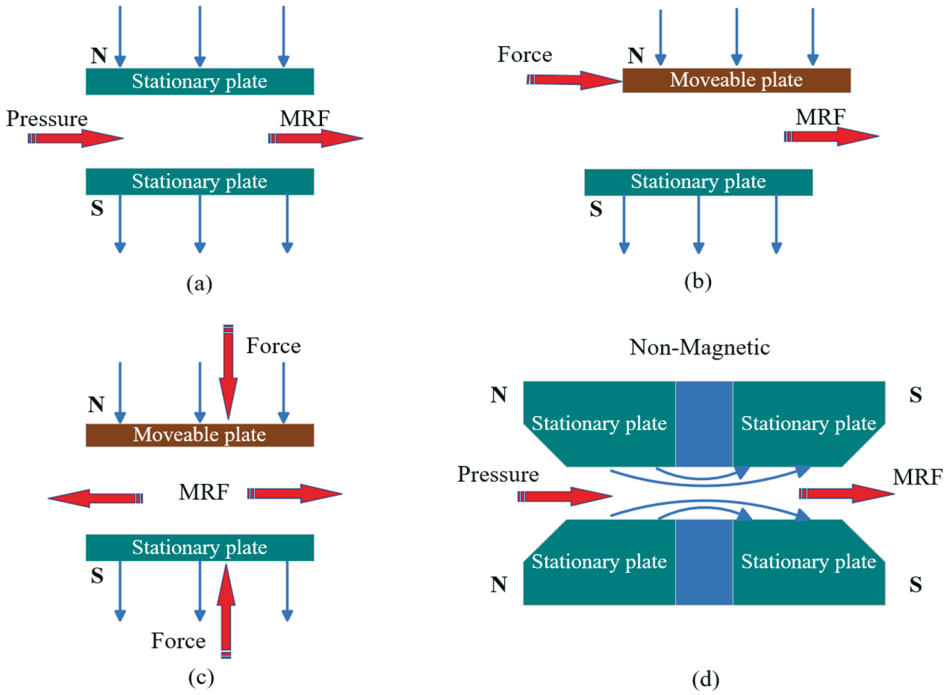

Fig. 3 Working mode of MR fluid (a) flow (valve) mode (b) shear mode (c) squeeze mode (d) pinch mode

Due to the inherent nonlinear hysteresis characteristics of MR dampers, it is necessary to establish a model and effective control strategy that can accurately describe the characteristics of MR dampers, so that their controllable characteristics can be fully utilised in practical applications. In this study, different types of models and control strategies are compared and summarised. The paper is organized as follows. Section 1 introduces the structure of an MR damper and the composition, characteristics, and working mode of the MR fluid. A detailed analysis of parametric and non-parametric models is given in Section 2. The control strategies related to two categories, i.e., the model-based control strategy and the soft computation-based control strategy, are introduced in Section 3. Section 4 summarises the main conclusions and puts forward some suggestions for the future research of the MR damper.

2. MR damper model

Due to the nonlinear hysteresis characteristics of force-displacement and force-velocity relationships of MR dampers [34], it is critical to develop accurate models of MR dampers to maximise their unique performance [35]. So far, various models have been established to simulate the behaviour of MR dampers. Based on different modelling approaches, MR damper models can be categorised into parametric models and nonparametric models [36].

2.1 Parametric model

Parametric modelling describes the device as a collection of linear or nonlinear springs, dampers, and other physical elements [37], where the MR damper is treated as a theoretical shock absorber composed of ideal mechanical elements [38].

Table 1 MR damper model

	Model	Schematic diagram	Equation	References
a	Bingham model	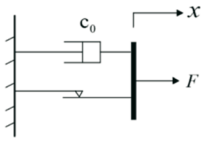	$F = f_c \cdot \mathrm{sgn}(\dot{x}) + c_0\dot{x}$	Stanway et al.1987 [39]
b	Nonlinear Bingham hysteretic model	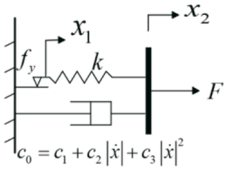	$F = \begin{cases} kx_1 + \left(c_1 + c_2\lvert\dot{x}_2\rvert + c_3\lvert\dot{x}_2\rvert^2\right)\dot{x}_2 + f_0 & , \\ \lvert kx_1\rvert \le f_y & \\ f_y\mathrm{sgn}(\dot{x}_2) + \left(c_1 + c_2\lvert\dot{x}_2\rvert + c_3\lvert\dot{x}_2\rvert^2\right)\dot{x}_2 + f_0 & , \\ \lvert kx_1\rvert \ge f_y & \end{cases}$	Zhang et al.2013 [49]
c	Fractional derivative Bingham model	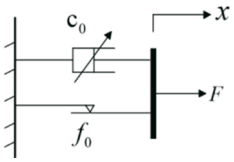	$F = f_c\,\mathrm{sgn}\left(x^{(\varphi)}\right) + c_0 x^{(\varphi)} + f_0$	Li et al.2015 [50]
d	Bouc-Wen model	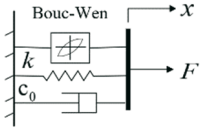	$F = c_0\dot{x} + k(x - x_0) + \alpha z$ $\dot{z} = -\gamma\lvert\dot{x}\rvert z\lvert z\rvert^{n-1} - \beta\dot{x}\lvert z\rvert^n + A\dot{x}$	Ismail et al.2009 [55]
e	Modified Bouc-Wen model	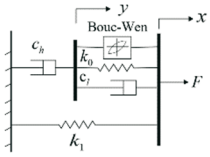	$F = c_h\dot{y} + k_1(x - x_0)$ $\dot{z} = -\gamma\lvert\dot{x} - \dot{y}\rvert z\lvert z\rvert^{n-1} - \beta(\dot{x} - \dot{y})\lvert z\rvert^n + A(\dot{x} - \dot{y})$ $\dot{y} = \frac{1}{c_h + c_l}\left(\alpha z + c_0\dot{x} + k_0(x - y)\right)$	Spencer et al.1997 [41]
f	The nonlinear bi-viscous model	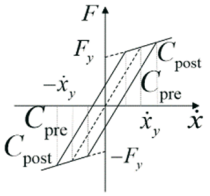	$F(t) = \begin{cases} C_{post}\dot{x} + F_y & x \ge \dot{x}_y \\ C_{pre}\dot{x} & -\dot{x}_y \ge \dot{x} \ge \dot{x}_y \\ C_{post}\dot{x} - F_y & \dot{x} \le -\dot{x}_y \end{cases}$	Snyder et al.2001 [63]
g	Generalised hysteretic bi-viscous operators model	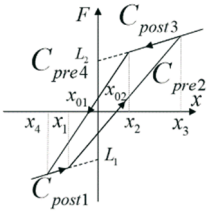	$F = \begin{cases} C_{post1}x - L_1 & x \le x_1 & \dot{x} > 0 \\ C_{pre2}(x - x_{01}) & x_1 \le x \le x_3 & \dot{x} > 0 \\ C_{post3}x + L_2 & x_3 \le x & \dot{x} > 0 \\ C_{post3}x + L_2 & x_2 \le x & \dot{x} < 0 \\ C_{pre4}(x - x_{02}) & x_4 \le x \le x_2 & \dot{x} < 0 \\ C_{post1}x - L_1 & x \le x_4 & \dot{x} < 0 \end{cases}$	Zhao et al.2018 [65]
h	Modified Dahl model	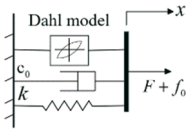	$F = kx + c_0 + f_d z - f_0$	Zhou et al.2002 [67]
i	Hyperbolic tangent function model	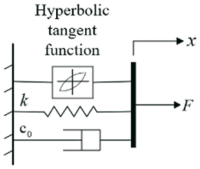	$F = c_0\dot{x} + kx + \alpha z + f_0$ $z = \tanh\left(\beta\dot{x} + \gamma\mathrm{sgn}(x)\right)$	Kwok et al.2006 [48]

	Model	Schematic diagram	Equation	References
j	Polynomial model	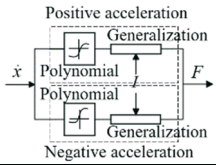	$F=\sum_{i=0}^{n}\left(b_i+c_i I\right)\dot{x}^i$	Choi et al.2001 [75]

2.1.1 Bingham model

To characterise the rheological behaviour of electrorheological (ER) dampers, Stanway et al. [39] developed the Bingham model in 1987, which includes a viscous damper placed parallel to the Coulomb friction unit [40], as shown in Table 1a. The force of the device is given by

$$F = f_c \cdot \operatorname{sgn}\left(\dot{x}\right) + c_0 \dot{x} \tag{1}$$

where F is the output damping force, f_c is the Coulomb friction force, sgn is the signum function, c_0 is the damping coefficient, $\dot{x}$ is the velocity. It should be noted that when the speed of the piston at any point is zero, the force applied is equal to the force generated in the friction device [41].

At present, the Bingham model finds extensive application in the modelling of both ER and MR dampers [42-46]. This model is relatively simple and easy to implement, which can accurately predict the magnitude of the damping force [47]. However, it does not fully take the pre-yield viscoelastic properties of the MR fluids into account, so it cannot completely describe the hysteresis behaviour of dampers [48]. Especially at low speeds, the performance is not satisfactory when hysteresis characteristics are displayed. To solve these problems, Zhang et al. [49] proposed a new nonlinear Bingham hysteretic model as shown in Table 1b, which can not only represent the hysteresis traits of the force-velocity relationship loop, but also describe the nonlinear behaviour at lower speeds. The force generated by the MR damper is written as

$$F=\begin{cases} kx_1+\left(c_1+c_2\left|\dot{x}_2\right|+c_3\left|\dot{x}_2\right|^2\right)\dot{x}_2+f_0 & , \\ \left|kx_1\right|\le f_y & \\ f_y\operatorname{sgn}\left(\dot{x}_2\right)+\left(c_1+c_2\left|\dot{x}_2\right|+c_3\left|\dot{x}_2\right|^2\right)\dot{x}_2+f_0 & , \\ \left|kx_1\right|\ge f_y & \end{cases} \tag{2}$$

where k is the equivalent stiffness of the MR damping spring element, x_1 is the Coulomb element displacement, c_1, c_2 and c_3 are the constant term, the primary term and the secondary term of the nonlinear damping coefficient of the MR damper, respectively, f_y is the yield force of the MR damper, and f_0 is the initial pre-tension.

Liu et al. [50] designed a fractional derivative Bingham model with fewer parameters. The model takes the changes of pre-yield and post-yield viscoelastic properties of the damper into account, so that the damping force-displacement and damping force-velocity relationships of the MR damper are well-fitted. The equation is described as

$$F = f_c \operatorname{sgn}\left(x^{(\varphi)}\right) + c_0 x^{(\varphi)} + f_0 \tag{3}$$

where $x^{(\varphi)}$ represents the φ order derivative of the displacement.

In addition, Guo et al. [51] constructed an extended Bingham model that can simultaneously characterise the hysteretic and bi-viscous behaviours of MR dampers [52, 53]. This model demonstrates superior accuracy compared to the Bingham model in

characterising the behaviours of dampers. The extended Bingham model of MR dampers is often expressed as

$$F = A_1 \tanh\left(A_3 \left(\dot{x} + \frac{V_0}{X_0} x \right) \right) + A_2 \left(\dot{x} + \frac{V_0}{X_0} x \right) \tag{4}$$

where A_1 is the dynamic yield force of the MR fluid, A_2 is the correlation parameter of the viscous damping coefficient after yield, A_3 is the correlation parameter of the viscous damping coefficient before yield, V_0 is the absolute value of the hysteresis critical velocity, X_0 is the absolute value of the hysteresis critical displacement, and x is the displacement.

2.1.2 Bouc-Wen model

In 1976, Wen [54] enhanced the hysteresis semi-physical model proposed by Bouc in 1971 [55]. As shown in Table 1d, the Bouc Wen model used to characterise the hysteresis characteristics of nonlinear components has been widely applied in many engineering fields. The Bouc-Wen model is written as

$$F = c_0 \dot{x} + k\left(x - x_0\right) + \alpha z \tag{5}$$

where z is governed by

$$\dot{z} = -\gamma |\dot{x}| z |z|^{n-1} - \beta \dot{x} |z|^n + A\dot{x} \tag{6}$$

where α is the scaling factor, γ, β and A are the model parameters, x_0 is the initial deflection of a linear spring, and z is the evolutionary variable.

Since the Bouc-Wen model can describe well the characteristics of force-displacement and force-velocity relationships of the MR dampers, it is widely used in the hysteretic simulation of MR dampers [56, 57]. However, this model has too many parameters, so Rodríguez et al. [58] normalized this model to eliminate the problem of over-parameterisation. To enhance the accuracy of predicting the damping response, Spencer et al. [41] developed an improved Bouc-Wen model which is shown in Table 1e and the damper force is given by

$$F = c_h \dot{y} + k_1\left(x - x_0\right) \tag{7}$$

where $\dot{z}$ and $\dot{y}$ are governed by

$$\dot{z} = -\gamma |\dot{x} - \dot{y}| z |z|^{n-1} - \beta\left(\dot{x} - \dot{y}\right)|z|^n + A\left(\dot{x} - \dot{y}\right) \tag{8}$$

$$\dot{y} = \frac{1}{c_h + c_l}\left(\alpha z + c_0 \dot{x} + k_0\left(x - y\right)\right) \tag{9}$$

where c_h and c_l are the viscous damping at high speed and the viscous damping at low speed, respectively, y is the internal displacement of the damper, k_0 is the stiffness at high speed, and k_1 is the stiffness of the accumulator.

Due to the large number of parameters, the computational efficiency of the improved Bouc-Wen model is relatively low. To address this issue, Rosli et al. [59] employed dynamic cuckoo and adaptive cuckoo search algorithms to optimise the improved Bouc-Wen model [60]. In 2007, Kwok et al. [34] used a strategy of adjusting velocity values when calculating

hysteresis variables and proposed an asymmetric Bouc Wen model. This model takes the asymmetric hysteresis phenomenon not mentioned in the initial Bouc Wen model into account, reduces the errors caused by the hysteresis phenomenon [61, 62], and improves the accuracy of the model. The damping force in this system is usually expressed as

$$F = c_0\dot{x} + kx + \alpha z - f_0 \tag{10}$$

$$\dot{z} = \left(A - \left(\beta + \gamma \operatorname{sgn}\left(z\dot{x}\right)\right)|z|^n\right)\dot{x} \tag{11}$$

$$\dot{x} \leftarrow \left(\dot{x} - \mu \operatorname{sgn}\left(x\right)\right) \tag{12}$$

where μ is the adjusted scale factor.

2.1.3 Bi-viscous model

The model mentioned above, such as the Bingham model [39], assumes that the fluid is rigid in the pre-yield condition and cannot describe the characteristics under the condition of low shear rate in practical applications. Therefore, Snyder et al. [63] employed the nonlinear double-viscous model developed by Stanway et al. [64] to characterise MR dampers, which assumed that the MR fluid exhibits plastic behaviour in both pre-yield and post-yield conditions. In addition, this model can capture the double-viscous behaviour of MR dampers [51]. The damping force is expressed as follows:

$$F\left(t\right) = \begin{cases} C_{post}\dot{x} + F_y & x \geq \dot{x}_y \\ C_{pre}\dot{x} & -\dot{x}_y \geq \dot{x} \geq \dot{x}_y \\ C_{post}\dot{x} - F_y & \dot{x} \leq -\dot{x}_y \end{cases} \tag{13}$$

where $F\left(t\right)$ is the output damping force at the time t, C_{post} and C_{pre} are the pre-yield and post-yield damping coefficients, respectively (C_{pre} should be assumed to be much larger than C_{post}), $\dot{x}_y$ is the yield velocity, and F_y is the yield force of the MR damper, which is represented by the yield force and the asymptotic intercept of the velocity and the force axis, as shown in Table 1f.

However, the above model can only represent the symmetric hysteresis characteristics. To describe the asymmetric hysteresis characteristics of MR dampers, Zhao et al. [65] proposed a model based on generalised hysteretic bi-viscous operators as shown in Table 1g. The modified model of MR dampers is expressed as

$$F = \begin{cases} C_{post1}x - L_1 & x \leq x_1 & \dot{x} > 0 \\ C_{pre2}\left(x - x_{01}\right) & x_1 \leq x \leq x_3 & \dot{x} > 0 \\ C_{post3}x + L_2 & x_3 \leq x & \dot{x} > 0 \\ C_{post3}x + L_2 & x_2 \leq x & \dot{x} < 0 \\ C_{pre4}\left(x - x_{02}\right) & x_4 \leq x \leq x_2 & \dot{x} < 0 \\ C_{post1}x - L_1 & x \leq x_4 & \dot{x} < 0 \end{cases} \tag{14}$$

where L_1 and L_2 are the constants derived from the projection of the yield curve at $x = 0$.

However, the model cannot accurately describe the characteristics of MR dampers when the damping force saturation value is reached. Therefore, scholars use the improved particle swarm optimisation algorithm to carry out a weighted superposition and optimise the weights to achieve an online adjustment of model parameters and weights. The model combines the advantages of parametric modelling and non-parametric modelling and can better simulate the characteristics of MR dampers.

2.1.4 Dahl model

The Dahl model [66] was proposed to describe the bearing friction, but it was found that this model could also be used to describe the hysteretic characteristics of dampers. In 2002, Zhou et al. [67] developed an improved Dahl model as shown in Table 1h, which required fewer model parameters to be determined than the commonly used Bouc-Wen model. The damping force is shown as follows:

$$F = kx + c_0 + f_d z - f_0 \tag{15}$$

where z is governed by

$$\dot{z} = \gamma \dot{x}\left(1 - z\,\mathrm{sgn}\left(\dot{x}\right)\right) \tag{16}$$

where f_d is the adjustable Coulomb friction force.

Considering the asymmetry of the hysteresis loop of the MR damper experiment, Garcia-Banos et al. [68] proposed an improved viscous Dahl model based on the viscous Dahl model proposed by Ikhouane et al. [69]. The model combines the change of friction coefficient and displacement, and the theoretical hysteresis provided by the model closely matches the actual hysteresis. The equations describing the damper model are as follows:

$$F\left(t\right) = F_v\left(t\right) + F_d\left(t\right) \tag{17}$$

$$\begin{aligned} \dot{w}\left(t\right) &= \rho\left(\dot{x}\left(t\right) - \left|\dot{x}\left(t\right)\right| w\left(t\right)\right) \\ -1 &\le w\left(0\right) \le 1 \end{aligned} \tag{18}$$

where $F_v\left(t\right)$ represents the viscous friction, $F_d\left(t\right)$ represents the dry friction, ρ is a constant greater than zero, and w is an internal variable.

2.1.5 Hyperbolic tangent function-based model

In 2006, Kwok et al. [48] constructed a model based on the hyperbolic tangent function as shown in Table 1i. Since the model only contains one hyperbolic tangent function, this function has high efficiency in parameter identification and control. However, there were some differences between the simulation results and experimental data. The model is written by

$$F = c_0 \dot{x} + kx + \alpha z + f_0 \tag{19}$$

$$z = \tanh\left(\beta \dot{x} + \gamma\,\mathrm{sgn}\left(x\right)\right) \tag{20}$$

Meng et al. [70] developed a new model based on the arc-tangent function, which has fewer parameters and a clearer physical definition. Subsequently, Zhang et al. [71] further improved the model by analysing the sensitivity of each parameter to the model output using neural network methods. The damping force is expressed as

$$F = a_1 \tanh\left(a_2\left(\dot{x}+\alpha x\right)\right) + a_3\left(\dot{x}+\alpha x\right) + f_0 \tag{21}$$

where a_1 is the scale factor, a_2 and a_3 are the damping coefficients affecting the regional variation of the pre-yield and the post-yield region, respectively.

2.1.6 Quasi-static magic formula model

The quasi-static model has been introduced to determine the hysteretic characteristics of MR dampers [72]. Although the model is simple and computationally efficient, it cannot effectively predict the relationship between the damping force and the velocity under dynamic excitation. In 2021, Bui et al. [73] employed the mechanical parameters of the magic formula to characterise the dynamic response of MR dampers, thereby compensating for the limitations of quasi-static models [74, 75]. The model introduces two new independent parameters S_a and S_b in the hysteresis component, which enables the model to describe high asymmetric hysteresis behaviour. The model is depicted by

$$F = F_{QS} \cdot \sin\left(A \arctan\left(\gamma(1-\beta)\, p + B \arctan\left(\gamma p\right)\right)\right) \tag{22}$$

where p is derived by

$$p = \begin{cases} \dot{x} + S_a x \;\; for\; \ddot{x} \geq 0 \\ \dot{x} + S_b x \;\; for\; \ddot{x} < 0 \end{cases} \tag{23}$$

where F_{QS} is the damping force obtained by the quasi-static model, p is the displacement variable dependent on the acceleration direction, and B, S_a and S_b are the model parameters.

It can be seen from the above analysis that the simplicity of the parametric models is usually achieved by decreasing the number of parameters. However, this simplicity is based on the cost of reducing the model accuracy. In addition, the MR damper is too idealised, and the influence of the temperature factor is usually ignored in parametric models. The adaptability and accuracy of the model can be improved by considering the temperature factors.

2.2 Nonparametric model

Nonparametric modelling is another modelling method for MR dampers. Being different from the parametric modelling method, it is based on the test data analysis and the working principle of the components, and it uses analytical expressions to describe the characteristics of the components [37].

2.2.1 Polynomial model

The polynomial model is a widely used mathematical model, which has great advantages in dealing with nonlinear problems [76]. In 2000, Choi et al. [77] constructed a polynomial model to represent the hysteresis behaviour of the damper as shown in Table 1j. The model partitioned the hysteresis characteristics into two domains i.e., positive acceleration and negative acceleration [78], and these domains were represented by a polynomial function based on the power of piston velocity. The parameters in this model are insensitive to the input current, which makes the model more convenient for implementing an open-loop control system. The model is depicted by

$$F = \sum_{\mathrm{i}=0}^{\mathrm{n}} \left(\mathrm{b_i} + \mathrm{c_i} I\right) \dot{x}^i \tag{24}$$

where b_i and c_i are the coefficients obtained by the experiment and I is the current.

The polynomial model proposed by Choi et al. [77] is a higher-order polynomial model. In 2015, Arias-Montiel et al. [79] investigated a lower-order (second-order) polynomial model as shown by the following expression:

$$F = \begin{cases} \left(b_{2p} + c_{2p} I\right)\dot{x}^2 + \left(b_{1p} + c_{1p} I\right)\dot{x} + \left(b_{0p} + c_{0p} I\right) & \text{for } a > 0 \\ \left(b_{2n} + c_{2n} I\right)\dot{x}^2 + \left(b_{1n} + c_{1n} I\right)\dot{x} + \left(b_{0n} + c_{0n} I\right) & \text{for } a > 0 \end{cases} \tag{25}$$

where a , b_i and c_i are the coefficients obtained by the experiment.

This model is simpler than the higher-order polynomial model and requires less hardware to process data in the control system. However, the peak stage is less precise in predicting the damping force compared to the higher-order polynomial model.

2.2.2 Fuzzy model

The fuzzy model describes the nonlinear system with a set of IF-THEN fuzzy rules [80]. It analyses the input and output data through appropriate algorithms and finally obtains an MR damper model represented by a polynomial equation. In 2009, Du et al. [81] established a fuzzy model of the MR damper using the Takagi-Sugeno (T-S) fuzzy modelling technology to reduce the impact of earthquakes on building structures. The fuzzy rules are represented as follows:

$$\text{IF } \xi_1 \text{ is } M_{i1} \text{ and ... and } \xi_s \text{ is } M_{is}$$
$$\text{THEN } f_i(t) = a_{1i} x(t) + a_{2i} \dot{x}(t) + b_{1i} u(t) \ , \ i = 1, ..., r$$

where the damping force in this system is expressed as

$$F(\mathrm{t}) = \sum_{\mathrm{i}=1}^{\mathrm{r}} \lambda_{\mathrm{i}}(\xi) f_i(t) = \sum_{\mathrm{i}=1}^{\mathrm{r}} \lambda_{\mathrm{i}}(\xi)\left(a_{1i} x(t) + a_{2i} \dot{x}(t) + b_{1i} u(t)\right) \tag{26}$$

where M_{ij} is the fuzzy set, r is the fuzzy rule number, $u(t)$ is the instruction signal, ξ is the premise variable, $f_i(t)$ is the fuzzy rule output force, and a_{1i} , a_{2i} and b_{1i} are the linear result parameters.

Some scholars combined a neural network and a fuzzy model to form a neural fuzzy model, such as the fuzzy model mentioned in literature [82, 83], which can well describe the characteristics of MR dampers, but high-impact loads may fail to predict the peak force. To solve this problem, Arsava et al. [84] proposed a neural fuzzy model, which can effectively simulate nonlinear behaviours under high-impact loads, and the accuracy of the peak prediction force exceeds 97%.

2.2.3 Neural network model

The neural network model can approximate any function with any accuracy and is usually composed of three layers of neurons, i.e., the input layer, the hidden layer, and the output layer, where the hidden layer can systematically learn nonlinear relations [85]. When a neural network is used to model an MR damper, it can predict the best damping force based on the response or excitation. This model can also be called a positive neural network model [86]. According to the ideal damping force predicted by a trained neural network model, a suitable control voltage or current can be generated [87], which is also called the inverse neural network model [88].

Non-parametric models typically use functional approximation or data-driven methods to describe the dynamic behaviour of MR dampers [89]. Unlike parametric models, they do not rely on specific physical parameters, but fit based on actual data, which can better describe the

system behaviour. However, this modelling method requires a large amount of experimental data for training and learning and the preliminary preparation is more complicated.

3. Control strategy of an MR damper

The semi-active control system of an MR damper includes three parts, i.e., a sensor, a controller and an actuator. The controller calculates the information from the sensor, and the actuator achieves precise control of the output damping force of the MR damper through the calculation results [38]. It is noteworthy that the MR damper cannot directly regulate the magnitude of the damping force output. Typically, a conversion algorithm or an MR damping inverse model are employed to manipulate the voltage or current signal to control the output damping force [90]. The control strategies can be divided into the model-based control and the soft computing-based control.

3.1 Model-based control strategy

The model-based control is a method of using relatively accurate mathematical expressions to describe physical characteristics of controlled objects and perform a corresponding control on them. The model-based control of an MR damper is shown in Figure 4.

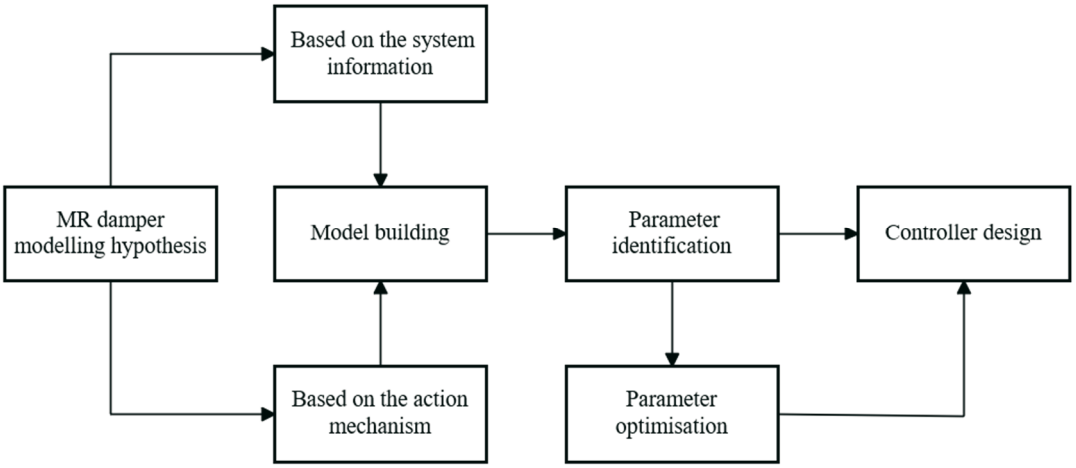

Fig. 4 Flow chart of model-based control strategy

3.1.1 Clipped optimal control

In 1996, Dyke et al. [91] proposed the clipped optimal control (COC) algorithm, which utilised acceleration feedback to optimise the force by adjusting the control voltage of an MR damper [92, 93]. When the MR damper provides optimal damping force (i.e., $F = F_{\mathrm{c}}$), the output voltage remains at the present level. If the resulting damping force is less than the predicted optimal force and both forces have the same sign, the voltage should be increased to the maximum level. When the force produced by the MR damper exceeds the optimal force, the command voltage is reset to zero. This relationship is incorporated into the clipped optimal control method defined by

$$V = V_{\max} H\left(\left(F_{\mathrm{c}} - F\right)F\right) \tag{27}$$

where V is the command voltage, F_{c} is the expected optimal control force, and $H(\cdot)$ is the Heaviside step function.

The acceleration data required for this control method is easy to obtain, which has been proven to be a simple and reliable method [94]. However, this approach does not take the interaction between the actuator dynamics and the control structure into account. In view of this fact, Du et al. [95] developed a semi-active control method based on the COC theory, which realized the soft contact technology of a manipulator arm collision buffer using an MR damper and reduced the contact risk of the manipulator arm during work. Chaudhuri et al. [96] devised a control algorithm combining the linear quadratic Gaussian design and the COC for structural shock absorption, which makes it easier to obtain the optimal voltage required by the damper compared with the traditional optimal control algorithm.

3.1.2 Decentralized output feedback polynomial control

The decentralized output feedback polynomial control method was developed by Cha Y-J in 2011 based on the relationship between the interstory drift, the interstory velocity, and the optimal control signal of the MR damper [97]. This method has excellent results in reducing the response of bridge systems [98], where the voltage is determined by

$$V = \left(d_1 + d_2 x + d_3 x^2 + d_3 x^3\right) + \left(e_1 + e_2 x + e_3 x^2 + e_3 x^3\right) \tag{28}$$

where d_i and e_i are the optimal coefficients of the governing equation.

3.1.3 Sliding mode control

Lee et al. [99] developed a discrete-time continuous sliding mode control algorithm for semi-active control systems of MR dampers. Distinguished from the traditional sliding mode control algorithm, the improved algorithm estimates the controlling force based on the feedback of velocity, acceleration, and current controlling force rather than by calculating the restoring force and ground excitation [100]. This algorithm is very suitable for structures with elastic and inelastic characteristics. Luong et al. [101] proposed a control method based on the sliding mode control, which considered uncertain factors, such as aircraft weight and falling speed, and effectively improved the impact energy absorption rate of the aircraft during landing. Zhang et al. [102] investigated a synovial environment shock absorption method based on quasizero stiffness to reduce the impact of ambient vibration on robot operation accuracy, which has a good shock absorption ability under different working conditions Bashir et al. [103] investigated semi-active automotive suspension systems with integrated MR fluid dampers and proposed an advanced proportional-integral differential sliding mode control (A-PIDSMC). The A-PIDSMC uses the dynamic response of the controlled object to calculate the desired damping force and compare it with the actual force to predict the control voltage, which is mathematically defined by

$$V = \begin{cases} V_{\max}, & \theta > V_{\max} \\ V_{\min}, & \theta < V_{\min} \\ \theta, & Otherwise \end{cases} \tag{29}$$

where θ is governed by

$$\theta = G\left(F_c - HF_a\right)\operatorname{sgn}\left(F_a\right) \tag{30}$$

where F_a is the actual damping force, and the values of H and G are decided by using the trial and error method.

Compared with a single proportional-integral-derivative (PID) controller and the sliding mode control (SMC), the input voltage of the A-PIDSMC is relatively continuous and stable in the same conditions, which improves the ride comfort and safety of the vehicle.

3.1.4 Lyapunov control algorithm

The Lyapunov control algorithm is based on the Lyapunov stability theory [104-106]. The basic idea of the algorithm is to prove the stability of the system by constructing a Lyapunov function and designing a controller according to the derivative of the Lyapunov function. Nagarajaiah et al. [107] adopted the nonlinear Lyapunov control algorithm which has good robustness. The performance of MR dampers is defined by

$$c=\begin{cases} c_{\max}\left(\omega_n x_a+\dot{x}_a\right)\dot{x}_r>0 \\ c_{\min}\left(\omega_n x_a+\dot{x}_a\right)\dot{x}_r<0 \end{cases} \tag{31}$$

where $c_{\max}$ and $c_{\min}$ are maximum and minimum damping coefficients, respectively, $\omega_n=\sqrt{k}/m$, x_a is the absolute displacement, and $\dot{x}_r$ is the relative velocity.

3.1.5 Bang-bang control

The bang-bang control was established by McClamroch et al. [108] and applied to ER dampers [109]. Aly [110, 111] proposed an improved bang-bang control algorithm motivated by the quasi bang-bang controller, where the output voltage value is set to $0-V_{\max}$ defined by

$$V=\begin{cases} \gamma_c V_{\max}, & If\ \ \mathrm{sgn}(x)=1,\ \mathrm{sgn}(\dot{x})=1 \\ \beta_c V_{\max}, & If\ \ \mathrm{sgn}(x)=-1,\ \mathrm{sgn}(\dot{x})=-1 \\ A_c V_{\max}, & If\ \ \mathrm{sgn}(x)=1,\ \mathrm{sgn}(\dot{x})=-1 \\ V_{\max}, & Otherwise \end{cases} \tag{32}$$

where γ_c, β_c and A_c are the parameters and the value ranges from 0~1.

3.1.6 Backstepping control

The backstepping control method is suitable for dealing with uncertainty [112]. Zapateiro et al. [113] proposed a backstepping control method of the semi-active suspension system, where the control law is expressed as

$$V=-\frac{\left(x_w-x_{weq}\right)\left(1+h_1h_2\right)+\left(h_1+h_2\right)\dot{x}_w+f-g\left(k_x\dot{x}+k_{wa}\omega\right)}{k_{wb}\omega g}\forall g\neq 0, \\ otherwise\ \ f_{mr}=0 \tag{33}$$

where ω is the variable of hysteresis dynamics, x_w and $\dot{x}_w$ are the angular position and the angular velocity, respectively, k_x, k_{wa} and k_{wb} are the parameters of the control hysteresis linearity, x_{weq} is the equilibrium point of the system, and f_{mr} is the MR damper model.

3. 2 Soft computing-based control strategy

The soft computing techniques simulate biochemical processes of intelligent systems in nature and ensure the property of robustness [114-116], which is suitable for dealing with the modelling and control of MR systems.

3.2.1 Neural network control

The feedforward neural network (FNN) (Figure 5) transmits the information from the input layer to the middle layer and then to the output layer [117]. Wei et al. [118] used the instantaneous variable constructed by the Hilbert transform to express the instantaneous characteristics of the excitation and further improved the accuracy of the FNN MR damper model. In addition, the model adopted an indirect modelling method for reducing the amount of data required for training the model, and the positive neural network model and the inverse neural network model are defined by

$$F(t)=FNN\begin{bmatrix} x(t),x(t-1).....x(t-N);\dot{x}(t),\dot{x}(t-1).....\dot{x}(t-N); \\ d(t),d(t-1).....d(t-N); \\ s(t),s(t-1).....s(t-N);p(t),p(t-1).....p(t-N); \\ i(t),i(t-1).....i(t-N);\theta \end{bmatrix} \tag{34}$$

where N represents the time span considered by the model corresponding to the input vector, s is the instantaneous frequency, p is the instantaneous phase, i is the impressed current, d is the envelope curve, and θ represents the weight and bias in the FNN structure.

The inverse neural network model can be written as

$$\tilde{i}_s(t)\begin{cases} \tilde{i}_s(t-1) & \left|F_T(t)-\tilde{F}_T(t)\right|\le\Delta F \\ \tilde{i}_s(t-1)+\dfrac{\left|F_T(t)\right|-\left|\tilde{F}_T(t)\right|}{\left|\tilde{F}_{\max}(t)\right|-\left|\tilde{F}_T(t)\right|}\left(i_{\max}-\tilde{i}_s(t-1)\right) & \left|F_T(t)-\tilde{F}_T(t)\right|>\Delta F and\left|F_T(t)\right|\ge\left|\tilde{F}_T(t)\right| \\ \tilde{i}_s(t-1)-\dfrac{\left|\tilde{F}_T(t)\right|-\left|F_T(t)\right|}{\left|\tilde{F}_T(t)\right|-\left|\tilde{F}_{\min}(t)\right|}\left(\tilde{i}_s(t-1)-i_{\min}\right) & \left|F_T(t)-\tilde{F}_T(t)\right|>\Delta F and\left|F_T(t)\right|<\left|\tilde{F}_T(t)\right| \end{cases} \tag{35}$$

where $F_T(t)$ is the target control force, $\tilde{F}_T(t)$ is the virtual target force, and $\tilde{i}_s(t)$ is the predicted current.

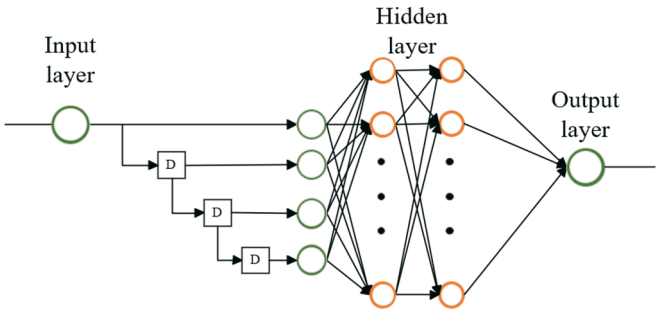

Fig. 5 Structure of FNN

Unlike FNNs, recurrent neural networks (RNNs) can feed output from a model back into its input layer [119], which enables them to address the aforementioned issue. The structure of an RNN is shown in Figure 6.

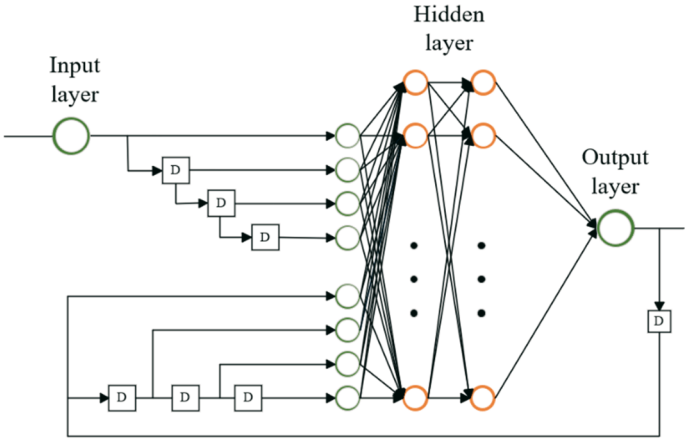

Fig. 6 Structure of RNN

In 2004, Wang et al. [120] first proposed an MR damper controller based on an RNN inverse recognition dynamic model. Compared with FNNs, the damping force generated by the predicted voltage can more accurately track the damping force generated by the target voltage [121], where the positive neural network model and the inverse neural network model are defined as follows.

The positive neural network model can be expressed as

$$\hat{F}(t+1)=NN\begin{bmatrix}\hat{F}(t),\hat{F}(t-1).....\hat{F}(t-O_F+1);\\ v(t),v(t-1).....v(t-I_v+1);\\ x(t),x(t-1).....x(t-I_x+1)\end{bmatrix} \tag{36}$$

where the neural network has I_v+I_x inputs and an output, $\hat{F}(t)$ is the predicted damping force, and O_F is the number of delays that the output of the neural network feeds back to the input layer.

The inverse neural network model can be defined as

$$\hat{V}(t+1)=NN\begin{bmatrix}\hat{v}(t),\hat{v}(t-1).....\hat{v}(t-O_v+1);\\ F(t),F(t-1).....F(t-I_F+1);\\ x(t),x(t-1).....x(t-I_x+1)\end{bmatrix} \tag{37}$$

where the neural network has I_F+I_x inputs and an output, $\hat{V}(t)$ is the predicted voltage, and O_v is the number of delays in the neural network model.

The back propagation neural network (BPNN) uses the backpropagation learning algorithm to improve connection weights of FNNs, which can realize arbitrary nonlinear mapping from input to output [122]. In 2013, Fu et al. [123] investigated a semi-active control algorithm of an MR damper based on a BPNN and a radial basis function neural network, which is combined with the skyhook control strategy. The experiments showed that this method can achieve a better shock absorption effect and improve the ride comfort. The method is expressed by the following formula:

$$i_t = NN\begin{bmatrix} F(t) & F(t-1) \\ x(t) & x(t-1) \\ \dot{x}(t) & \dot{x}(t-1) \end{bmatrix} \tag{38}$$

When using BPNNs to build forward and inverse models of MR dampers, they are usually optimised using appropriate algorithms. For example, Xu et al. [124] developed an optimised BPNN based on the artificial bee colony algorithm, which has higher computational efficiency and accuracy than the traditional BPNN. An optimisation method combining a BPNN and a particle swarm algorithm was proposed by Hu et al. [125]. It improved the magnetic field utilisation rate of the designed MR damper. Compared with that of the originally designed MR damper without using this method, the output damping force was increased by 91.1% and the adjustable range of the damping force was also increased by 40.0% under the same 1.8A current, which greatly improves the performance of the damper. Yan et al. [126] adopted the optimal genetic algorithm to optimise the initial weight and threshold to make its prediction more accurate.

3.2.2 Fuzzy control

The fuzzy logic theory is well-suited for controlling time-varying, nonlinear, and purely lagging systems [127, 128]. A semi-active fuzzy control strategy of MR dampers is developed in [129] and the control performance of the peak displacement ratio and the peak acceleration is superior to the COC method [91]. Das et al. [130] investigated a fuzzy logic control algorithm based on the fuzzification of MR damper characteristics, where the positive fuzzy model and the inverse fuzzy model are defined by (39) and (40), respectively:

$$F = W_1F_1 + W_2F_2 + ... + W_iF_i + ... + W_{n-1}F_{n-1} + W_nF_n \tag{39}$$

$$V = W_1V_1 + W_2V_2 + ... + W_iV_i + ... + W_{n-1}V_{n-1} + W_nV_n \tag{40}$$

where

$$\sum W_i = 1, \quad i = 1, 2, 3.....n \tag{41}$$

where W_i is the weight.

Fuzzy control relies on a set of fuzzy rules without the necessity of constructing a precise mathematical model of a controlled system [131]. However, it requires complex controller parameter adjustment. At present, the Takagi-Sugeno-Kang fuzzy inference system [132] and a fuzzy neural network [133] were proposed to solve this problem.

3.2.3 Support vector machines

The support vector machines (SVMs) can map the nonlinear relationship between factors related to the characteristics of MR dampers into a high-dimensional feature space and transform the nonlinear problem into a linear problem [134]. Shi et al. [135] proposed a control method of the MR damper based on SVMs and took the influence of temperature into account, which is very rare in the existing MR damper models and control methods. But a temperature rise is inevitable due to the coil energisation or the friction of particles in the fluid. The effect of temperature on MR dampers was considered in the literature [136, 137] and the structure is

shown in Figure 7. Compared with the BPNN without considering the effect of temperature, this method has better generalisation and approximation ability.

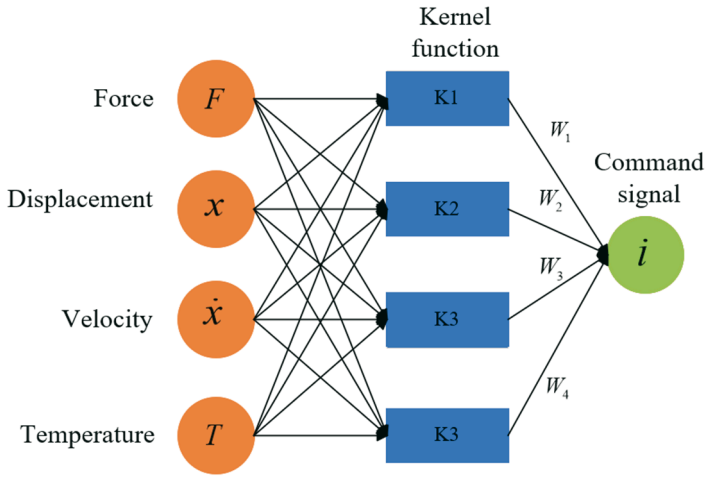

Fig. 7 SVM damper model considering temperature effect

4. Conclusions

In this paper, the existing models and control strategies of MR dampers are reviewed and their merits and limitations are analysed. The following conclusions can be drawn:

(1) The reported parametric modelling of an MR damper is mostly limited to inherent nonlinear nature caused by hysteresis characteristics of the force-displacement and force-velocity relationships. Such models thus cannot fully describe important effects associated with variations in many non-modelling factors.

(2) The non-parametric modelling method can improve the accuracy of the model; the complexity and computational burden of the models make the design of a closed-loop controller difficult.

(3) The effectiveness of the model-based control strategies relies on the accuracy of the controlled model, while the effectiveness of the soft computation-based control strategies is primarily influenced by data quality and adequacy.

The quality and applicability of MR damper models strongly depend on the representation of the force-displacement and force-velocity relationships. Therefore, further systematic efforts are needed to derive descriptions of the hysteresis characteristics of force displacement and force velocity so as to achieve a reliable MR damper model. On this basis, more intelligent theories will be adopted to achieve precise control.

Acknowledgement

This research was funded by the National Natural Science Foundation of China in 2021, grant number: 62073298; Key R&D projects in Henan Province, grant number: 232102221036; Key Scientific Research Projects of Doctoral Fund of Zhengzhou University of Light Industry, grant number: 2019BSJJ002. Henan Foreign Scientist Studio under grant GZS2023011.

Conflicts of interest

The authors declare that there are no conflicts of interest regarding the publication of this paper.

REFERENCES

[1] Sehovic, J.; Filipovic, I.; Pikula, B. Experimental Determination of Non-Linear Characteristics of the Passenger Vehicle Suspension System, *Transactions of FAMENA* **2020**, 44(2), 13-22. https://doi.org/10.21278/TOF.44202

[2] Yuan, R.; Yang, Y.; Su, C.; et al. Research on Vibration Reduction Control Based on Reinforcement Learning, *Advances in Civil Engineering* **2021**, 2021, 1-18. https://doi.org/10.1155/2021/7619214

[3] Ferdaus, M.; Rashid, M.; Bhuiya, M. Development of an Advanced Semi-Active Damper Using Smart Fluid, *Advanced Materials Research* **2014**, 939, 615-622. https://doi.org/10.4028/www.scientific.net/AMR.939.615

[4] Ferdaus, M.; Rashid, M.; Hasan, M.; Rahman, M. Optimal design of Magneto-Rheological damper comparing different configurations by finite element analysis, *Journal of Mechanical Science and Technology* **2014**, 28(9), 3667-3677. https://doi.org/10.1007/s12206-014-0828-5

[5] Munyaneza, O.; Sohn, J. Modeling and control of hybrid MR seat damper and whole body vibration evaluation for bus drivers, *Journal of Low-Frequency Noise Vibration and Active Control* **2022**, 41(2), 659-675. https://doi.org/10.1177/14613484211063095

[6] Paciello, V.; Pietrosanto, A. Magnetorheological Dampers: A New Approach of Characterization, *IEEE Transactions on Instrumentation & Measurement* **2011**,60(5), 1718-1723. https://doi.org/10.1109/TIM.2010.2102391

[7] Giorgetti, A.; Baldanzini, N.; Biasiotto, M.; Citti, P. Design and testing of a MRF rotational damper for vehicle applications, *Smart Materials and Structures* **2010**, 19(6), Article ID 065006. https://doi.org/10.1088/0964-1726/19/6/065006

[8] Rahman, M.; Ong, Z. C.; Julai, S.; Ferdaus M. M.; Ahamedet, R. A review of advances in magnetorheological dampers: their design optimization and applications, *Journal of Zhejiang University-Science A* **2017**, 18(12), 991-1010. https://doi.org/10.1631/jzus.A1600721

[9] Rabinow, J. The magnetic fluid clutch, *Electrical Engineering* **1948**, 67(12), 1167-1167. https://doi.org/10.1109/EE.1948.6444497

[10] Shetty, B. G.; Prasad, P. S. S. Rheological Properties of a Honge Oil-based Magnetorheological Fluid used as Carrier Liquid, *Defence Science Journal* **2011**, 61(6), 583-589. https://doi.org/10.14429/dsj.61.331

[11] Kumbhar, B. K.; Patil, S. R.; Sawant, S. M. Synthesis and characterization of magneto-rheological (MR) fluids for MR brake application, *Engineering Science & Technology An International Journal* **2015**, 18(3), 432-438. https://doi.org/10.1016/j.jestch.2015.03.002

[12] Jamadar, M. E. H.; Devikiran, P.; Desai, R. M.; Kumar, H.; Joladarashi, S. Real-time testing and thermal characterization of a cost-effective magneto-rheological (MR) damper for four-wheeler application, *Journal of the Brazilian Society of Mechanical Sciences and Engineering* **2023**, 45(2), 2-26. https://doi.org/10.1007/s40430-023-04035-x

[13] Zhang, G.; Chen, J. Y.; Zhang, Z.; et al. Analysis of magnetorheological clutch with double cup-shaped gap excited by Halbach array based on finite element method and experiment, *Smart Materials & Structures* **2022**, 31(7), Article ID 075008. https://doi.org/10.1088/1361-665X/ac701a

[14] He, Y. C.; Liang, G. Q.; Xue, B.; Peng, Z. Z.; Wei, Y. T. A unified MR damper model and its inverse characteristics investigation based on the neuro-fuzzy technique, *International Journal of Applied Electromagnetics and Mechanics* **2019**, 61(2), 225-245. https://doi.org/10.3233/JAE-180114

[15] Elsaady, W.; Oyadiji, S. O.; Nasser, A. A review on multi-physics numerical modelling in different applications of magnetorheological fluids, *Journal of Intelligent Material Systems and Structures* **2020**, 31(16), 1855-1897. https://doi.org/10.1177/1045389X20935632

[16] Lee, T. H.; Kang, B. H.; Choi, S. B. A quasi-static model for the pinch mode analysis of a magnetorheological fluid flow with an experimental validation, *Mechanical systems and signal processing* **2019**, 134, Article ID 106308. https://doi.org/10.1016/j.ymssp.2019.106308

[17] Kubik, M.; Goldasz, J.; Machacek, O.; Strecker Z.; Sapinski, B. Magnetorheological fluids subjected to non-uniform magnetic fields experimental characterization, *Smart Materials and Structures*, **2023**, 32(3), Article ID 035007. https://doi.org/10.1088/1361-665X/acb473

[18] Goncalves, F. D.; Carlson, J. D. An alternate operation mode for MR fluids-magnetic gradient pinch, *Journal of Physics : Conference Series* **2009**, 149(1), Article ID 012050. https://doi.org/10.1088/1742-6596/149/1/012050

[19] Sapinski, B.; Goldasz, J. Development and performance evaluation of an MR squeeze-mode damper, *Smart Materials and Structures* **2015**, 24(11), Article ID 115007. https://doi.org/10.1088/0964-1726/24/11/115007

[20] Chooi, W. W.; Oyadiji, S. O. Design, modelling and testing of magnetorheological (MR) dampers using analytical flow solutions, *Computers & Structures* **2008**, 86(3-5), 473-482. https://doi.org/10.1016/j.compstruc.2007.02.002

[21] Savaia, G.; Panzani, G.; Corno, M.; Cecconi, J.; Savaresi, S. M. Hammerstein–Wiener modelling of a magneto-rheological dampers considering the magnetization dynamics, *Control Engineering Practice* **2021**, 112(5), Article ID 104829. https://doi.org/10.1016/j.conengprac.2021.104829

[22] Vishwakarma, P. N.; Mishra, P.; Sharma, S. K. Characterization of a magnetorheological fluid damper a review, Materials Today: Proceedings 2022, 56(5), 2988-2994. https://doi.org/10.1016/j.matpr.2021.11.143

[23] Jiang, R. L.; Rui, X. T.; Wei, M.; et al. A Phenomenological Model of Magnetorheological Damper Considering Fluid Deficiency, *Journal of Sound and Vibration* **2023**, 562, Article ID 117851. https://doi.org/10.1016/j.jsv.2023.117851

[24] Ahammed, R.; Hasan, M. Z. An FEA and CFD coupled numerical analysis approach for characterizing magneto-rheological (MR) grease damper, *Sādhanā* **2023**, 48(3), Article ID 164. https://doi.org/10.1007/s12046-023-02196-y

[25] Li, Y.; Yang, X. L.; Zhu, J. H.; Zhou, Y. M. Design and Performance Study of Hybrid Channel-valved Magnetorheological Dampers, *Journal of Magnetics* **2023**, 28(1), 6-15. https://doi.org/10.4283/JMAG.2023.28.1.006

[26] Brandão, F. D. S.; Miguel, L. F. F. A New Methodology for Optimal Design of Hybrid Vibration Control Systems (MR+ TMD) for Buildings under Seismic Excitation, *Shock and Vibration* **2023**, 2023. https://doi.org/10.1155/2023/8159716

[27] Wang, M. X.; Pang, H.; Luo, J. B.; Liu, M. H. On an enhanced back propagation neural network control of vehicle semi-active suspension with a magnetorheological damper, *Transactions of the Institute of Measurement and Control* **2023**, 45(3), 512-523. https://doi.org/10.1177/01423312221118224

[28] Jalali, H. H.; Farzam, M. F.; Gavgani, S. A. M.; Bekdas, G. Semi-active control of buildings using different control algorithms considering SSI, *Journal of Building Engineering* **2023**, 67. https://doi.org/10.1016/j.jobe.2023.105956

[29] Zhang, H. L.; Cheng, K. Y.; Wang, E. R.; Rakheja, S.; Su, C. Y. Nonlinear Behaviors of a Half-car Magneto-Rheological Suspension System under Harmonic Road Excitation, *IEEE Transactions on Vehicular Technology* **2023**, 72(7), 8592-8600. https://doi.org/10.1109/TVT.2023.3244586

[30] Baheti, A. S.; Matsagar, V. A. Wind and Seismic Response Control of Dynamically Similar Adjacent Buildings Connected Using Magneto-Rheological Dampers, *Infrastructures* **2022**, 7(12). https://doi.org/10.3390/infrastructures7120167

[31] Eshkevari, S. S.; Eshkevari, S. S.; Sen, D.; Pakzad, S. N. Active structural control framework using policy-gradient reinforcement learning, *Engineering Structures* **2023**, 274. https://doi.org/10.1016/j.engstruct.2022.115122

[32] Amirmojahedi, M.; Shojaee, S.; Hamzehei-Javaran, S. A fuzzy based intelligent scheme for enhancing the performance of the optimal controllers by online weighting matrix selection in seismically excited nonlinear buildings, *Engineering Structures* **2023**, 294. https://doi.org/10.1016/j.engstruct.2023.116738

[33] Abdulateef, W. S.; Hejazi, F. Fuzzy logic based adaptive vibration control system for structures subjected to seismic and wind loads, *Structures* **2023**, 55, 1507-1531. https://doi.org/10.1016/j.istruc.2023.06.108

[34] Kwok, N. M.; Ha, Q. P.; Nguyen, M. T.; Li, J.; Samali, B. Bouc-Wen model parameter identification for a MR fluid damper using computationally efficient GA, *Isa Transactions* **2007**, 46(2), 167-179. https://doi.org/10.1016/j.isatra.2006.08.005

[35] Ruiz-Lopez, J. A.; Hidalgo-Alvarez, R.; Vicente, J. A micromechanical model for magnetorheological fluids under slow compression, *Rheologica Acta* **2016**, 55(3), 215-221. https://doi.org/10.1007/s00397-016-0910-2

[36] Ahamed, R.; Ferdaus, M. M.; Li, Y. C. Advancement in energy harvesting magneto-rheological fluid damper: A review, *Korea-Australia Rheology Journal* **2016**, 28(4), 355-379. https://doi.org/10.1007/s13367-016-0035-2

[37] Wang, D. H.; Liao, W. H. Magnetorheological fluid dampers: a review of parametric modelling, *Smart Materials and Structures* **2011**, 20(2), Article ID 023001. https://doi.org/10.1088/0964-1726/20/2/023001

[38] Lv, H. Z.; Zhang, S. S.; Sun, Q.; Chen, R.; Zhang, W. J. The Dynamic Models, Control Strategies and Applications for Magnetorheological Damping Systems: A Systematic Review, *Journal of Vibration Engineering & Technologies* **2020**, 9(1), 131-147. https://doi.org/10.1007/s42417-020-00215-4

[39] Stanway, R.; Sproston, J. L.; Stevens, N. G. Non-linear modelling of an electro-rheological vibration damper, *Journal of Electrostatics* **1987**, 20(2), 167-184. https://doi.org/ 10.1016/0304-3886(87)90056-8

[40] Zapateiro, M.; Luo, N. S.; Taylor, E.; Dyke, S. J. Modeling and identification of a class of MR fluid foam dampers, *Smart Structures and Systems* **2010**, 6(2), 101-113. https://doi.org/10.12989/sss.2010.6.2.101

[41] Spencer Jr, B. F.; Dyke, S. J.; Sain, M. K.; Carlson, J. D. Phenomenological Model for Magnetorheological Dampers, *Journal of Engineering Mechanics* **1997**, 123(3), 230-238. https://doi.org/10.1061/(ASCE)0733-9399(1997)123:3(230)

[42] Marath, A. P.; Khot, S. M.; Nagler, J. Development of Low-Cost Optimal Magneto-rheological Damper for Automotive Application, *Journal of Vibration Engineering & Technologies* **2022**, 10(5), 1831-1850. https://doi.org/10.1007/s42417-022-00486-z

[43] Soltane, S.; Montassar, S.; Ben Mekki, O.; El Fatmi, R. A hysteretic Bingham model for MR dampers to control cable vibrations, *Journal of Mechanics of Materials and Structures* **2015**, 10(2), 195-206. https://doi.org/10.2140/jomms.2015.10.195

[44] Chen, K.; Yu, X. P.; Wang, H. S.; et al. Modeling of a Bingham model of a magnetorheological damper considering stochastic uncertainties in their geometric variables, *Journal of Theoretical and Applied Mechanics* **2021**, 59(1), 53-65. https://doi.org/10.15632/jtam-pl/128811

[45] Makris, N.; Burton, S. A.; Taylor, D. P. Electrorheological damper with annular ducts for seismic protection applications, *Smart Materials and Structures* **1996**, 5(5), 551-564. https://doi.org/10.1088/0964-1726/5/5/005

[46] Marinca, V.; Ene, R. D.; Bereteu, L. Application of the optimal homotopy asymptotic method to nonlinear Bingham fluid dampers, *Open Physics* **2017**, 15(1), 620-626. https://doi.org/10.1515/phys-2017-0072

[47] Choi, Y. T.; Wereley, N. M.; Jeon, Y. S. Semi-Active Vibration Isolation Using Magnetorheological Isolators, *Journal of Aircraft* **2005**, 42(5), 1244-1251. https://doi.org/10.2514/1.7919

[48] Kwok, N. M.; Ha, Q. P.; Nguyen, T. H.; Li, J.; Samali, B. A novel hysteretic model for magnetorheological fluid dampers and parameter identification using particle swarm optimization, *Sensors and Actuators A Physical* **2006**, 132(2), 441-451. https://doi.org/10.1016/j.sna.2006.03.015

[49] Zhang, Z. X.; Huang, F. L. A New Magneticrheological Damper Nonlinear Bingham Hysteretic Model and ANSYS Implementation, *Applied Mechanics & Materials* **2013**, 351-352, 1146-1151. https://doi.org/10.4028/www.scientific.net/AMM.351-352.1146

[50] Li, X. M.; Li, H. Y.; Huang, Y. J. Fractional derivative Bingham model of MR damper, *Journal of Mechanical & Electrical Engineering* **2015**, 32(3), 338-342.

[51] Guo, S. Q.; Yang, S. P.; Pan, C. Z. Dynamic Modeling of Magnetorheological Damper Behaviors, *Journal of Intelligent Material Systems and Structures* **2006**, 17(1), 3-14. https://doi.org/10.1177/1045389X06055860

[52] Basargan, H.; Mihály, A.; Gáspár, P.; Sename, O.; An LPV-based online reconfigurable adaptive semi-active suspension control with MR damper, *Energies* **2022**, 15(10). https://doi.org/10.3390/en15103648

[53] Josee, M.; Kazima, S.; Turabimana, P. Review of semi-active suspension based on Magneto-rheological damper, *Engineering Perspective* **2021**, 4(1), 38-51. https://doi.org/10.29228/eng.pers.50853

[54] Wen, Y. K. Method for Random Vibration of Hysteretic Systems, *Journal of the Engineering Mechanics Division* **1976**, 102(2), 249-263. https://doi.org/10.1061/JMCEA3.0002106

[55] Ismail, M.; Ikhouane, F.; Rodellar, J. The hysteresis Bouc-Wen model, a survey, *Archives of Computational Methods in Engineering* **2009**, 16(2), 161-188. https://doi.org/10.1007/s11831-009-9031-8

[56] Dominguez, A.; Sedaghati, R.; Stiharu, I. Modeling and application of MR dampers in semi-adaptive structures, *Computers & Structures* **2008**, 86(3-5), 407-415. https://doi.org/10.1016/j.compstruc.2007.02.010

[57] Xie, H. L.; Li, G. C.; Li, F. Modeling of Magnetorheological Damper and Fuzzy PID Control of Intelligent Bionic Leg with Meniscus, in *2019 WRC Symposium on Advanced Robotics and Automation (WRC SARA)* **2019**, pp. 387-393. https://doi.org/10.1109/WRC-SARA.2019.8931965

[58] Rodríguez, A.; Iwata, N.; Ikhouane, F.; Rodellar, J. Model identification of a large-scale magnetorheological fluid damper, *Smart Materials & Structures* **2009**, 18(1). https://doi.org/10.1088/0964-1726/18/1/015010

[59] Rosli, R.; Mohamed, Z. Optimization of modified Bouc–Wen model for magnetorheological damper using modified cuckoo search algorithm, *Journal of Vibration and Control* **2021**, 27(17-18), 1956-1967. https://doi.org/10.1177/1077546320951383

[60] Urda, P.; Pérez, J.; Carabias, E.; Cabrera, J. A.; Castillo, J. J. Design and testing of a steering damper for motorcycles based on a shear-thickening fluid, *Smart Materials and Structures* **2022**, 31(9). https://doi.org/10.1088/1361-665X/ac8325

[61] Zhou, L. A.; Zhang, S. L. Modeling and parameter identification of asymmetric restoring force of reinforced concrete shear walls, *Advances in Mechanical Engineering* **2023**, 15(8). https://doi.org/10.1177/16878132231192226

[62] Cao, Y. M.; Chen, W. J.; Ma, H.; et al. Dynamic modeling and experimental verification of clamp–pipeline system with soft nonlinearity, *Nonlinear Dynamics* **2023**, 111(17725-17748). https://doi.org/10.1007/s11071-023-08814-y

[63] Snyder, R. A.; Kamath, G. M.; Wereley, N. M. Characterization and Analysis of Magnetorheological Damper Behavior Under Sinusoidal Loading, *AiAA Journal* **2001**, 39(7), 1240-1253. https://doi.org/10.2514/3.14862

[64] Stanway, R.; Sproston, J. L.; El-Wahed, A. K. Applications of electro-rheological fluids in vibration control: a survey, *Smart Materials & Structures* **1996**, 5(4), 464-482. https://doi.org/10.1088/0964-1726/5/4/011

[65] Zhao, X. L.; Wu, S. J.; Pan, H. P. A Hybrid Model of Magnetorheological Dampers Based on Generalized Hysteretic Biviscous Operators, *Journal of Intelligent Material Systems & Structures* **2018**, 29(14), 2979-2985. https://doi.org/10.1177/1045389X18781051

[66] Dahl, P. R. Solid Friction Damping of Mechanical Vibrations, *AIAA Journal* **1976**, 14(12), 1675-1682. https://doi.org/10.2514/3.61511

[67] Zhou, Q.; Zhai, W. L. Two Mechanic Models for Magnetorheological Damper and Corresponding Test Verification, *Earthquake Engineering and Engineering Dynamics* **2002**, 22(4), 144-150. https://doi.org/10.1016/j.engstruct.2013.03.006

[68] Garcia-Banos, I.; Ikhouane, F.; Aguirre-Carvajal, N. An asymmetric-friction based model for magnetorheological dampers, *IFAC-PapersOnLine* **2018**, 20(1), 14076-14081. https://doi.org/10.1016/j.ifacol.2017.08.1844

[69] Ikhouane, F.; Dyke, S. J. Modeling and identification of a shear mode magnetorheological damper, *Smart Materials and Structures* **2007**, 16(3), 605-616. https://doi.org/10.1088/0964-1726/16/3/007

[70] Meng, F. X.; Zhou, J. Modelling and experimental investigation of a squeeze mode magnetorheological damper, *International Journal of Applied Electromagnetics and Mechanics* **2019**, 61(4), 549-561. https://doi.org/10.3233/JAE-190008

[71] Zhang, S. G.; Shi, W. K.; Chen, Z. Y. Modeling and Parameter Identification of MR Damper Considering Excitation Characteristics and Current, *Shock and Vibration*, **2021**, 2021. https://doi.org/10.1155/2021/6691650

[72] Hong, S. R.; John, S.; Wereley, N. M.; Choi, Y. T.; Choi, S. B. A Unifying Perspective on the Quasi-steady Analysis of Magnetorheological Dampers, *Journal of Intelligent Material Systems and Structures* **2008**, 19(8), 959-976. https://doi.org/10.1177/1045389X07082949

[73] Bui, Q. D.; Bai, X. X.; Nguyen, Q. H. Dynamic modeling of MR dampers based on quasi–static model and Magic Formula hysteresis multiplier, *Engineering Structures* **2021**, 245. https://doi.org/10.1016/j.engstruct.2021.112855

[74] Lv, H. Z.; Sun, Q.; Zhang, W. J. A comparative study of four parametric hysteresis models for magnetorheological dampers, *Actuators* **2021**, 10(10). https://doi.org/10.3390/act10100257

[75] Parlak, Z.; Sahin, I.; Parlak, N. One-way coupled numerical model utilizing Viscoelastic Maxwell model for MR damper, *Journal of Intelligent Material Systems and Structures* **2022**, 33(19), 2391-2404. https://doi.org/10.1177/1045389X221085657

[76] Xu, B.; Li, J.; Dyke, S. J.; Deng, B. C.; He, J. Nonparametric identification for hysteretic behavior modeled with a power series polynomial using EKF-WGI approach under limited acceleration and unknown mass, *International Journal of Non-Linear Mechanics* **2020**, 119. https://doi.org/10.1016/j.ijnonlinmec.2019.103324

[77] Choi, S. B.; Lee, S. K.; Park, Y. P. A Hysteresis Model for The Field-Dependent Damping Force of a Magnetorheological Damper, *Journal of Sound and Vibration* **2001**, 245(2), 375-383. https://doi.org/10.1006/jsvi.2000.3539

[78] Li, W. F.; Dong, X. M.; Yu, J. Q.; Xi, J.; Pan, C. W. Vibration control of vehicle suspension with magneto-rheological variable damping and inertia, *Journal of Intelligent Material Systems and Structures* **2021**, 32(13), 1484-1503. https://doi.org/10.1177/1045389X20983885

[79] Arias-Montiel, M.; Florean-Aquino, K. H.; Francisco-Agustin, E.; et al. Experimental characterization of a magnetorheological damper by a polynomial model, in *2015 International Conference on Mechatronics, Electronics and Automotive Engineering (ICMEAE)* **2015**, pp. 128-133. https://doi.org/10.1109/ICMEAE.2015.31

[80] Taimoor, M.; Lu, X.; Shabbir, W.; Sheng, C. Y. Neural network observer based on fuzzy auxiliary sliding-mode-control for nonlinear systems, *Expert Systems with Applications* **2023**, 237. https://doi.org/10.1016/j.eswa.2023.121492

[81] Du, H. P.; Zhang, N. Model-based Fuzzy Control for Buildings Installed with Magneto-rheological Dampers, *Journal of Intelligent Material Systems and Structures* **2009**, 20(9), 1091-1105. https://doi.org/10.1177/1045389X09102148

[82] Priyandoko, G.; Baharom, M. Z. PSO-Optimised Adaptive Neuro-fuzzy System for Magneto-rheological Damper Modelling, *International Journal of Applied Electromagnetics and Mechanics* **2013**, 41(3), 301-312. https://doi.org/10.3233/JAE-121615

[83] Zeinali, M.; Mazlan, S. A.; Abd Fatah, A. Y.; Zamzuri, H. A phenomenological dynamic model of a magnetorheological damper using a neuro-fuzzy system, *Smart Materials and Structures* **2013**, 22(12), Article ID 125013. https://doi.org/10.1088/0964-1726/22/12/125013

[84] Arsava, K. S.; Kim, Y. Modeling of Magnetorheological Dampers under Various Impact Loads, *Shock and Vibration* **2015**, 2015, Article ID 905186. https://doi.org/10.1155/2015/905186

[85] Yakhni, M. F.; Ali, M. N.; El-Gohary, M. A. Magnetorheological damper voltage control using artificial neural network for optimum vehicle ride comfort, *Journal of Mechanical Engineering and Sciences* **2021**, 15(1), 7648-7661. https://doi.org/10.15282/jmes.15.1.2021.03.0603

[86] Wei, S. L.; Wang, J.; Ou, J. P. Experimental study on inverse model-based force tracking control of MR damper, *Shock and Vibration* **2020**, 2020, Article ID 8813024. https://doi.org/10.1155/2020/8813024

[87] Bhaiya, V.; Bharti, S. D.; Shrimali, M. K.; Datta, T. K. Velocity Tracking Control Algorithm for Semiactive Control of Building Frames, *ASPS Conference Proceedings* **2022**, 1, 653-658. https://doi.org/10.38208/acp.v1.566

[88] Chang, C. C.; Zhou, L. Neural Network Emulation of Inverse Dynamics for a Magnetorheological Damper, *Journal of Structural Engineering* **2002**, 128(2), 231-239. https://doi.org/10.1061/(ASCE)0733-9445(2002)128:2(231)

[89] Abdelhamed, M.; Ata, W. G.; Salem, A. M.; Khafagy, A. Z. Effect of modified bouc-wen model parameters on the dynamic hysteresis of magnetorheological dampers, *IOP Conference Series: Materials Science and Engineering* **2020**, 973, Article ID 012020. https://doi.org/10.1088/1757-899X/973/1/012020

[90] Sarrafan, A.; Zareh, S. H.; Khayyat, A. A. A.; Zabihollah, A. Neuro-fuzzy control strategy for an offshore steel jacket platform subjected to wave-induced forces using magnetorheological dampers, *Journal of Mechanical Science & Technology* **2012**, 26(4), 1179-1196. https://doi.org/10.1007/s12206-012-0212-2

[91] Dyke, S. J.; Spencer, B. F.; Sain, M. K.; Carlson, J. D. Modeling and control of magnetorheological dampers for seismic response reduction, *Smart Materials and Structures* **1996**, 5(5), 565-575. https://doi.org/10.1088/0964-1726/5/5/006

[92] Sharma, S. K.; Sharma, R. C.; Choi, Y.; Jaesun, J. S. Modelling and Dynamic Analysis of Adaptive Neuro-Fuzzy Inference System-Based Intelligent Control Suspension System for Passenger Rail Vehicles Using Magnetorheological Damper for Improving Ride Index, *Sustainability* **2023**, 15(16). https://doi.org/10.3390/su151612529

[93] Diep, B. T.; Nguyen, Q. H.; Le, T. D. Design and control of 2-DoF joystick using MR-fluid rotary actuator, *Journal of Intelligent Material Systems and Structures* **2022**, 33(12), 1562-1573. https://doi.org/10.1177/1045389X211063947

[94] Aziz, M. A.; Aminossadati, S. M. State-of-the-art developments of bypass Magnetorheological (MR) dampers: A review, *Korea-Australia Rheology Journal* **2021**, 33(3), 225-249. https://doi.org/10.1007/s13367-021-0018-9

[95] Du, X. P.; Chen, H.; Liu, Z. J.; Wang, C. Semi-active control of space manipulator soft contacting based on magnetorheological rotational damper, *Proceedings of the Institution of Mechanical Engineers Part C Journal of Mechanical Engineering Science* **2016**, 230(14), 2390-2398. https://doi.org/10.1177/0954406215594827

[96] Chaudhuri, P.; Manikanan, R. Semi-active Control of Structures Using Adaptive LQG based Clipped Optimal Controlled Magnetorheological Damper, in *2023 IEEE IAS Global Conference on Renewable Energy and Hydrogen Technologies (GlobConHT)* **2023**, 1-3. https://doi.org/10.1109/GLOBCONHT56829.2023.10087403

[97] Cha, Y. J.; Agrawal, A. K. Decentralized output feedback polynomial control of seismically excited structures using genetic algorithm, *Structural Control and Health Monitoring* **2013**, 20(3), 241-258. https://doi.org/10.1002/stc.486

[98] Cha, Y. J.; Agrawal, A. K.; Friedman, A.; et al. Performance validations of semiactive controllers on large-scale moment-resisting frame equipped with 200-kN MR damper using real-time hybrid simulations, *Journal of Structural Engineering* **2014**, 140(10), Article ID 04014066. https://doi.org/10.1061/(ASCE)ST.1943-541X.0000982

[99] Lee, T. Y.; Chen, P. C. Experimental and Analytical Study of Sliding Mode Control for Isolated Bridges with MR Dampers, *Journal of Earthquake Engineering* **2011**, 15(4), 564-581. https://doi.org/10.1080/13632469.2010.524277

[100] Katebi, J.; Zadeh, S. M. Time delay study for semi-active control of coupled adjacent structures using MR damper, *Structural Engineering and Mechanics* **2016**, 58(6), 1127-1143. https://doi.org/10.12989/sem.2016.58.6.1127

[101] Luong, Q. V.; Jang, D. S.; Hwang, J. H. Robust Adaptive Control for an Aircraft Landing Gear Equipped with a Magnetorheological Damper, *Applied Sciences-Basel* **2020**. https://doi.org/10.3390/app10041459

[102] Zhang, L. X.; Zhao, C. M.; Qian, F.; Dhupia, J. S.; Wu, M. L. An Active Control with a Magnetorheological Damper for Ambient Vibration, *Machines* **2022**, 10(2). https://doi.org/10.3390/machines10020082

[103] Bashir, A. O.; Rui, X. T.; Abbas, L. K.; Zhou, Q. B. MR-damped vehicle suspension ride comfort enhancement based on advanced proportional-integral-differential sliding mode control, *Control Engineering and Applied Informatics* **2018**, 20(4), 11-21.

[104] Manna, S.; Akella, A. K.; Singh, D. K. Novel Lyapunov-based rapid and ripple-free MPPT using a robust model reference adaptive controller for solar PV system, *Protection and Control of Modern Power Systems* **2023**, 8(1), Article ID 13. https://doi.org/10.1186/s41601-023-00288-9

[105] Cetin, S.; Zergeroglu, E.; Sivrioglu, S.; Yuksek, I. A new semiactive nonlinear adaptive controller for structures using MR damper: Design and experimental validation, *Nonlinear Dynamics* **2011**, 66(4), 731-743. https://doi.org/10.1007/s11071-011-9946-0

[106] Bagherkhani, A.; Baghlani, A. Reliability assessment of MR fluid dampers in passive and semi-active seismic control of structures, *Probabilistic Engineering Mechanics* **2021**, 63. https://doi.org/10.1016/j.probengmech.2020.103114

[107] Nagarajaiah, S.; Narasimhan, S.; Agrawal, A.; Tan, P. Benchmark structural control problem for a seismically excited highway bridge—Part III: Phase II Sample controller for the fully base-isolated case, *Structural Control and Health Monitoring* **2009**, 16(5), pp. 549-563. https://doi.org/10.1002/stc.293

[108] McClamroch, N. H.; Gavin, H. P. Closed loop structural control using electrorheological dampers, in *Proceedings of 1995 American Control Conference-ACC'95* **1995**, 6, 4173-4177. https://doi.org/10.1006/jsvi.2002.5136

[109] Barroso, L. R.; Hunt, S.; Chase, J. G. Application of magneto-rheological dampers for multi-level seismic hazard mitigation of hysteretic structures, in *Proceedings of the 15th ASCE Engineering Mechanics Conference* **2002**, 2-5.

[110] Aly, A. M. Vibration Control of Buildings Using Magnetorheological Damper: A New Control Algorithm, *Journal of Engineering* **2013**, 2013. https://doi.org/10.1155/2013/596078

[111] Kumar, G.; Kumar, A.; Jakka, R. S. The Particle Swarm modified quasi bang-bang controller for seismic vibration control, *Ocean Engineering* **2018**, 166, 105-116. https://doi.org/10.1016/j.oceaneng.2018.08.002

[112] Basri, M. A. M.; Danapalasingam, K. A.; Husain, A. R. Design and optimization of backstepping controller for an underactuated autonomous quadrotor unmanned aerial vehicle, *Transactions of FAMENA* **2014**, 38(3), 27-44.

[113] Zapateiro, M.; Luo, N. S.; Harimi, H. R. Neural Network – Backstepping Control for Vibration Reduction in a Magnetorheological Suspension System, *Solid State Phenomena* **2009**, 147-149, 839-844. https://doi.org/10.4028/www.scientific.net/SSP.147-149.839

[114] Wu, Z.; Liao, H. C.; Lu, K. Y.; Zavadskas, E. K. Soft Computing Techniques and Their Applications in Intelligent Industrial Control Systems: A Survey, *International Journal of Computers Communications & Control* **2021**, 16(1), Article ID 4142. https://doi.org/10.15837/ijccc.2021.1.4142

[115] Dong, X. M.; Yu, M.; Liao, C. R.; Chen, W. M. Comparative research on semi-active control strategies for magneto-rheological suspension, *Nonlinear Dynamics* **2010**, 59(3), 433-453. https://doi.org/10.1007/s11071-009-9550-8

[116] Weber, F.; Bhowmik, S.; Hogsberg, J. Extended neural network-based scheme for real-time force tracking with magnetorheological dampers, *Structural Control & Health Monitoring* **2014**, 21(2), 225-247. https://doi.org/10.1002/stc.1569

[117] Chang, C. C.; Roschke, P. Neural Network Modeling of a Magnetorheological Damper, *Journal of Intelligent Material Systems and Structures* **1998**, 9(9), 755-764. https://doi.org/10.1177/1045389X9800900908

[118] Wei, S. L.; Wang, J.; Ou, J. P. Method for improving the neural network model of the magnetorheological damper, *Mechanical Systems and Signal Processing* **2021**, 149. https://doi.org/10.1016/j.ymssp.2020.107316

[119] Wang, Y. J.; Gu, J.; Yuan, L. Distribution network state estimation based on attention-enhanced recurrent neural network pseudo-measurement modeling, *Protection and Control of Modern Power Systems* **2023**, 8(1), Article ID 31. https://doi.org/10.1186/s41601-023-00306-w

[120] Wang, D. H.; Liao, W. H. Modeling and control of magnetorheological fluid dampers using neural networks, *Smart Materials and Structures* **2005**, 14(1), 111-126. https://doi.org/10.1088/0964-1726/14/1/011

[121] Guo, Y. Q.; Zhang, J.; He, D. Q.; Li, J. B. Magnetorheological elastomer precision platform control using OFFO-PID algorithm, *Advances in Materials Science and Engineering*, **2020**, https://doi.org/10.1155/2020/3025863

[122] Wang, W.; Zhang, J. F.; Wang, S.; Chen, X. W. Effective fault module localization in substation critical equipment: an improved ant colony optimization and back propagation neural network approach, *The Journal of Engineering* **2023**, 2023(10). https://doi.org/10.1049/tje2.12315

[123] Fu, J.; Yao, H. J.; Yu, M.; Peng, Y. X. An experimental model identification of magneto-rheological damper with neural network and its application in seat suspension system, in *Proceedings of the 32nd Chinese Control Conference* **2013**, 8769-8774.

[124] Xu, Q.; Chen, J. Y.; Liu, X. P.; Li, J.; Yuan, C. Y. An ABC-BP-ANN algorithm for semi-active control for Magnetorheological damper, *KSCE Journal of Civil Engineering* **2017**, 21(6), 2310-2321. https://doi.org/10.1007/s12205-016-0680-5

[125] Hu, G. L.; Qi, H. N.; Chen, M.; et al. Optimal design of magnetorheological damper with multiple axial fluid flow channels using BP neural network and particle swarm optimization methodologies, *International Journal of Applied Electromagnetics and Mechanics* **2021**, 67(3), 339-360. https://doi.org/10.3233/JAE-210089

[126] Yan, Y. Y.; Dong, L. L.; Han, Y.; Li, W. S. A general inverse control model of a magneto-rheological damper based on neural network, *Journal of Vibration and Control* **2022**, 28(7-8), 952-963. https://doi.org/10.1177/1077546320986380

[127] Rahmani, B.; Ziaiefar, A.; Hashemi, S. Output feedback-based adaptive fuzzy sliding mode control for seismic response reduction of base-isolated buildings, *ISA Transactions* **2022**, 126, 94-108. https://doi.org/10.1016/j.isatra.2021.07.021

[128] Caponetto, R.; Diamante, O.; Fargione, G.; Risitano, A.; Tringali, D. A soft computing approach to fuzzy sky-hook control of semiactive suspension, *IEEE Transactions on Control Systems Technology* **2003**, 11(6), 786-798. https://doi.org/10.1109/TCST.2003.819592

[129] Kumar, G.; Kumar, R.; Kumar, A. A Review of the Controllers for Structural Control, *Archives of Computational Methods in Engineering* **2023**, 30(6), 3977-4000. https://doi.org/10.1007/s11831-023-09931-y

[130] Das, D.; Datta, T. K.; Madan, A. Semiactive fuzzy control of the seismic response of building frames with MR dampers, *Earthquake engineering & structural dynamics* **2012**, 41(1), 99-118. https://doi.org/10.1002/eqe.1120

[131] Zhou, S.; Liu, J.; Wang, Z.; Sun, S. Research on Design Optimization and Simulation of Regenerative Braking Control Strategy for Pure Electric Vehicle Based on EMB Systems, *Transactions of FAMENA* **2023**, 47(4), 33-49. https://doi.org/10.21278/TOF.474045522

[132] Raeesi, F.; Azar, B. F.; Veladi, H.; Talatahari, S. An inverse TSK model of MR damper for vibration control of nonlinear structures using an improved grasshopper optimization algorithm, *Structures* **2020**, 26, 406-416. https://doi.org/10.1016/j.istruc.2020.04.026

[133] Zhang, H.; Zhang, R. J.; He, Q.; Liu, L. X. Variable Universe Fuzzy Control of High-Speed Elevator Horizontal Vibration Based on Firefly Algorithm and Backpropagation Fuzzy Neural Network, *IEEE Access* **2021**, 9, 57020-57032. https://doi.org/10.1109/ACCESS.2021.3072648

[134] Qian, C.; Yin, X. L.; Ouyang, Q. Modeling and parameter identification of the MR damper based on LS-SVM, *International Journal of Aerospace Engineering* **2021**, 2021. https://doi.org/10.1155/2021/6648749

[135] Shi, Y. F.; Feng, Z. M.; Zhou, Y.; Dong, Z. Z.; Zhao, H. Y. Research on modeling of magneto-rheological damping dynamic inverse model based on support vector machine, in *2019 14th IEEE International Conference on Electronic Measurement & Instruments (ICEMI)* **2019**, 768-778. https://doi.org/10.1109/icemi46757.2019.9101577

[136] Li, H. P.; Jnkkri, I.; Sarlin, E.; Chen, F. Temperature effects and temperature-dependent constitutive model of magnetorheological fluids, *Rheologica Acta* **2021**, 60(11), 719-728. https://doi.org/10.1007/s00397-021-01302-3

[137] Kariganaur, A. K.; Kumar, H.; Arun, M. Influence of temperature on magnetorheological fluid properties and damping performance, *Smart Materials and Structures* **2022**, 31(5). https://doi.org/10.1088/1361-665X/ac6346

Submitted: 22.11.2023

Accepted: 15.02.2024

Zhijun Fu[1]
Xiang Zhang[1]
Zhigang Zhang*[1]
Dengfeng Zhao[1]
Yuming Yin[2]
[1]Henan Key Laboratory of Intelligent Manufacturing of Mechanical Equipment, Zhengzhou University of Light Industry, Zhengzhou, 450000, China
[2] School of Mechanical Engineering, Zhejiang University of Technology, Hangzhou, 310023, China
*Corresponding author:
zhigangzhang@foxmail.com